The 5s−4d Rydberg States of C_2H_2 and C_2D_2 Studied by Resonant Multiphoton Ionization and Synchrotron Radiation: Structure and Stability

A. Campos,[†] S. Boyé,[‡] S. Douin,[‡] C. Fellows,[†] J. H. Fillion,[§] N. Shafizadeh,[‡] and D. Gauyacq*[,‡]

Laboratoire de Photophysique Moléculaire, Bâtiment 210, Université de Paris-Sud, 91405 Orsay Cédex, France, Instituto de Fisica, Universidade Federal Fluminense, Niteroi, Rio de Janeiro, Brazil, and Université de Cergy-Pontoise, 95806 Cergy Cédex, France

Received: April 24, 2001; In Final Form: July 19, 2001

The components of the 5s + 4d Rydberg complex of C_2H_2 and C_2D_2 have been studied by (3 + 1) photon ionization spectroscopy and fragment fluorescence excitation spectroscopy following synchrotron radiation VUV excitation. Thanks to the remarquable spectral resolution of the new synchrotron beam line SU5 at Super-ACO (12 mÅ in the range 248−65 nm), rotationally resolved spectra of Rydberg states of acetylene could be observed through their photofragment visible fluorescence. Unlike the lower 4s + 3d Rydberg complex, all Rydberg components of this complex exhibit rotational line widths typical of a 1−10 ps predissociation. The $^1\Phi_u$ 4dδ_g and $^1\Delta_u$ 4dπ_g components have been characterized for both isotopic species. The relative electronic band intensities of the REMPI spectra have been interpreted within a semi-united atom model and by taking into account predissociation.

I. Introduction

Photolysis of acetylene has been widely studied in many fields as combustion and astrophysics, in which it plays a crucial role as a source of highly reactive radicals. Photodecomposition of this molecule in the UV up to the far VUV domain has been investigated theoretically and experimentally, using lamps, lasers, and synchrotron radiation. Fragment formation has been analyzed by using laser-induced fluorescence (LIF),[1] fragment emission,[2] multiphoton ionization detection (REMPI),[3] and H-fragment translational spectroscopy.[4,5] When this molecule is excited by VUV photons below the first ionization limit, i.e., 11.4 eV, Rydberg states are primarily excited due to their very strong absorption cross section. As shown earlier by high-resolution absorption spectroscopic analysis performed by Herman and Colin,[6] most of these Rydberg states exhibit a very diffuse absorption structure due to predissociation. Therefore, these states can be considered as intermediate steps toward hydrocarbon radicals formation from acetylene photolysis. This photolysis is of special interest in some astrophysical media as circumstellar envelopes[7] or cometary atmospheres,[8] where the UV radiation field is still important up to the 13.6 eV cutoff energy. In this context, the understanding of the relaxation pathways of these Rydberg states over the excitation range 8−11.4 eV is an astrophysical issue to address.

The absorption spectrum of the Rydberg states converging to the ionic ground state $^2\Pi_u$ shows prominent s and d series, with various electronic components of $^1\Sigma_u^+$ and $^1\Pi_u$ symmetry.[6] Among these series, some show a moderate predissociation rate associated with resolved rotational structure while others show strong predissociation resulting in a completely diffuse structure. Among all the Rydberg states, the electronic components of the lowest Rydberg complex 3d + 4s have been the subject of thorough investigation, as they can be considered prototype states for all Rydberg series up to the ionization limit. Resonant multiphoton spectroscopy (3 + 1 REMPI) has been able to complete the absorption data by allowing observation of the 3dδ $^1\Phi_u$ component[9] and of the 3dπ $^1\Delta_u$ component.[10] Among all components of this 3d + 4s Rydberg complex, only the 3dπ $^1\Sigma_u^-$ remains a dark state due to its symmetry. In their REMPI analysis of the 3d + 4s complex of both C_2H_2 and C_2D_2, Fillion et al.[10] could quantitatively interpret the observed relative intensities and line widths of the various electronic components of the 3d complex: they simulated the 3-photon excitation intensities with first and third rank transition tensors on one hand, and introduced a predissociation rate for each electronic state, on the other hand. This predissociation rate could account for both the observed intensities and rotational line widths. More recently, this complex has been studied by laser VUV excitation and H-fragment translational spectroscopy.[4,5] Finally, a very precise ab initio calculation[11] has predicted the energy structure of this complex as well as the s−d mixing within the electronic components, in very good agreement with the REMPI observations of ref 10.

The next Rydberg complex 4d + 5s is not as well-known as the 3d + 4s complex. The absorption spectrum shows rotationally resolved origin bands corresponding to the upper I, 5sσ $^1\Pi_u$ and J, 4dδ $^1\Pi_u$ states, with an increased diffuseness for the J−X transition. Low-resolution REMPI, (3 + 1) photon spectra were recorded by Orlando et al.,[12] showing the corresponding three-photon I−X and J−X bands as broad features. The lack of rotational structure in these early REMPI spectra was mainly due to laser power broadening. Later on, Shafizadeh et al.[13] showed an overview of the high-resolution (3 + 1) REMPI spectra of the 3d + 4s and 4d+5s complexes and gave a rough estimate of the Rydberg states lifetimes derived from observed line widths in absorption and REMPI studies. Surprisingly, the J, 4dδ $^1\Pi_u$ state, which corresponds to the next member of the *n*dδ $^1\Pi_u$ series, does not exhibit such a strong

* To whom correspondence should be addressed. E-mail: dolores.gauyacq@ppm.u-psud.fr. Fax: 33 1 69 15 67 77.
[†] Universidade Federal Fluminense.
[‡] Université de Paris-Sud.
[§] Université de Cergy-Pontoise.

10.1021/jp0115392 CCC: $20.00
Published on Web 09/15/2001

predissociation as the first member, the H state, since it can be observed by REMPI (3 + 1) photon spectroscopy.

In the present work the 4d + 5s complex of C_2H_2 is investigated by using two excitation schemes, a one-photon VUV absorption or a three-photon excitation. The aim of this work is to understand the competition between the ionization and the dissociation channels when REMPI is used to investigate high Rydberg states of acetylene and to compare the different behaviors toward predissociation between the first two complexes of this molecule. The experiment using VUV one-photon excitation was performed with a synchrotron radiation source and by detecting both the absorption signal and the total fluorescence of the photofragments in the visible. The very high spectral resolution of the synchrotron line allowed us to observe rotationally resolved absorption. The REMPI spectra showed a new weak band previously unassigned and not observed by one-photon absorption. From the analysis of the C_2D_2 isotopomer, we could assign unambiguously this band to a new electronic component of the 4d + 5s complex. We finally present a rotational intensity simulation involving all the related electronic Rydberg components based on the semi-united atom model. In this model, the predissociation channel has been taken into account in a phenomenological way in order to fit both the decrease of the ionization signal and the observed line widths.

II. Experimental Section

The (3 + 1) REMPI experiments were performed in a magnetic bottle electron spectrometer, described elsewhere.[14] Acetylene, as well as its isotopomer C_2D_2, was introduced into a vacuum chamber through a 2 mm diameter hole. Typical background pressure was 10^{-5} mbar in the interaction region, so that an effusive beam condition allowed for moderate rotational cooling of the molecules. The total photoelectron signal was collected by a microchannel plate detection system, through an appropriate time gate selecting only the electrons produced by the (3 + 1) ionization process in acetylene, and accumulated over about 60 laser shots.

Tunable radiation was generated by an excimer (XeCl, LUMONICS PM 886) pumped dye laser (Lambda Physik FL2002) operating in the 360 nm spectral region (BMQ dye solution), with a bandwidth of 0.3 cm^{-1}. To minimize laser power broadening of the REMPI spectra, beam intensities were maintained at about 200 μJ per pulse and controlled during the scan by a micro joulemeter (Laser Precision Corporation RjP 700). The beam was focused into the ionization volume by a 150 mm focal length lens.

The experiment at the synchrotron radiation facility at Orsay (Super-ACO) was performed by using two beam lines, SA63 and SU5. The SA63 beam line is equipped with a 3 m Eagle normal incidence monochromator and a 1800 grooves/mm grating tuned in the 154−60 nm spectral region with a 0.08 nm resolution. In the experiment performed with this beam line, acetylene was introduced into a vacuum chamber by means of a stainless needle with a 100 μm internal diameter and was excited by the VUV beam close to the gas aperture.[15] The SU5 beam light, dispersed by a high-resolution 6.65 m Eagle off-plane normal incidence monochromator and a 2400 grooves/mm grating, was tuned in the 248−65 nm energy range with a resolution of about 12 mÅ.[16] Acetylene was introduced in a supersonic jet expansion through a 50 μm nozzle at right angle with the VUV beam. A background pressure of about 10^{-4} mbar was maintained in the vacuum chamber and a differential pumping system enabled to work without any window between the interaction chamber and the high-vacuum monochromator.

Two signals were simultaneously recorded: (i) The transmitted VUV light was recorded through the visible fluorescence of a coated sodium salicylate window and collected by a photomultiplier tube (Hamamatsu R928, spectral range 950−185 nm), providing then an absorption signal. (ii) The fluorescence from the excited fragments arising from the VUV photodissociation of acetylene was collected by a sensitive fluorescence detection device described in detail elsewhere.[17] The undispersed visible fluorescence was recorded by a photomultiplier tube (Hamamatsu R928), as a function of the VUV excitation wavelength.

III. Results and Discussion

A. Dissociation and Ionization Channels for the I $^1\Pi_u$ and J $^1\Pi$u Rydberg States. The two $^1\Pi_u$ Rydberg states of the 4s + 3d complex, namely the G and H states, exhibit very different lifetimes, as pointed out by Löffler et al.[18] and later on by Shafizadeh et al.[13] The lifetime of the H state, of about 30 fs, precludes observation of this state in the REMPI spectra observed with typical nanosecond laser power densities. According to ref 18, these two states exhibit equal H atom yields following VUV one-photon excitation, indicating that both states predissociate mainly into C_2H + H products, but within different time scales. Recently, dispersed fragment fluorescence, following VUV excitation from a synchrotron radiation source, was detected from these states, showing that the C_2H fragment is produced in the A state and fluoresces in both the visible and the infrared range.[15] In the 9.6−11.4 eV (IP) region, dissociation into excited C_2H fragments, with high bending excitation in the A state, resulting in visible fluorescence, becomes significant. As a consequence, the total visible fragment fluorescence spectrum completely reflects the absorption spectrum in this energy range.[15] This fluorescence signal can then be considered as an indirect measurement of the dissociation yield from the various Rydberg states lying in the high-energy region from 9.6 eV up to the IP (11.4 eV).

Nevertheless, this total fragment fluorescence does not tell about the detailed dissociation mechanism, which can vary from one Rydberg state to another. The insight of the dissociation dynamics could be understood in the energy region of the G and H states thanks to H-translational detection experiments.[4,5] In this experiment, two different mechanisms could be inferred, giving rise to different H-translational time-of-flight spectra depending on the excitation light polarization: (i) a slow mechanism in the picosecond time scale, leaving the C_2H fragment with large internal energy, in one hand, and (ii) a very fast dissociation within about 30 fs, leaving the C_2H fragment with less internal energy and no bending vibrational excitation on the other hand. Both mechanisms occur in the H state with a similar probability.

The fast dissociation is responsible for the broad spectral bandwidth of the H−X absorption spectrum as well as for the lack of ionization signal in the REMPI experiments. On the other hand, the observed dissociation dynamics of the G state appears to proceed in a different way: this state shows a negligible probability toward the fast dissociation channel. The slow dissociation channel dominates, leaving the C_2H fragment with large internal energy and high bending vibrational excitation.

In the absence of polarization studies, both mechanisms occur but cannot be distinguished experimentally, except for the fact that the fast predissociation channel leads to a significant spectral broadening, both by one-photon or by three-photon excitation. A large spectral broadening is indeed observed in the H−X

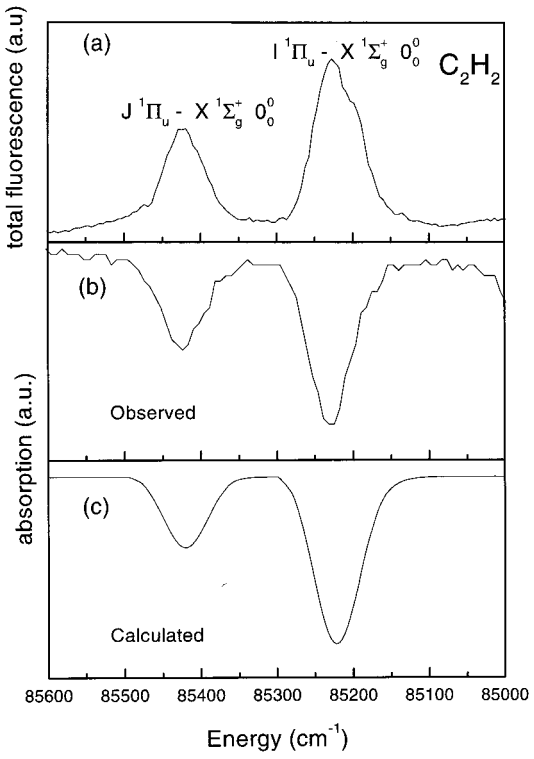

Figure 1. (a) Fluorescence excitation spectrum and (b) absorption spectrum of acetylene in the region of the I $^1\Pi_u$ and J $^1\Pi_u$ states, recorded at the synchrotron radiation with a resolution of 0.8 nm. (c) Absorption spectrum calculated in the semi-united atom approximation (see text).

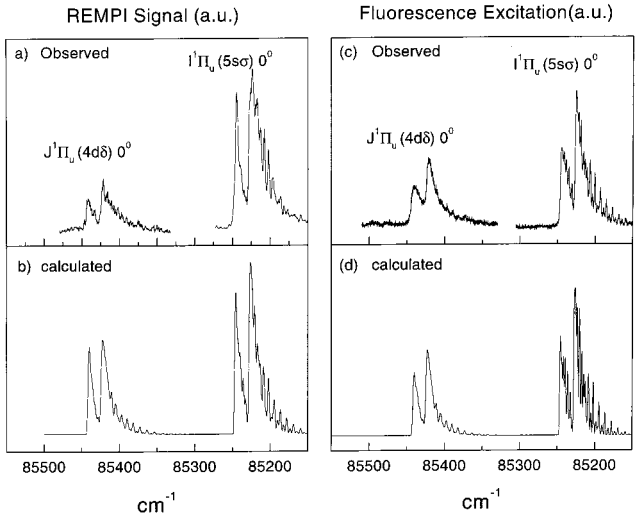

Figure 2. Origin band spectra of the I $^1\Pi_u$ and J $^1\Pi_u$ states: (a) REMPI spectrum (observed intensity normalized to the laser intensity I_{laser} by a $1/I_{laser}^3$ factor; (b) fragment fluorescence excitation spectrum (observed intensity normalized to the synchrotron beam intensity I_{synch} by a $1/I_{synch}$ factor); (c) calculated three-photon spectrum at 180 K with a rotational line width of 2 cm^{-1} for the I−X transition and 3 cm^{-1} for the J−X transition; (d) calculated one-photon absorption spectrum at 150 K with a rotational line width of 1.5 cm^{-1} for the I−X transition and 3 cm^{-1} for the J−X transition. The rotational B values for both I $^1\Pi_u$ and J $^1\Pi_u$ states have been fixed to the I $^1\Pi_u$ state B value[6], $B = 1.099\,55$ cm^{-1}.

VUV absorption band, while no such broadening is observed in the G−X absorption band, in agreement with Löffler et al. analysis.[5] In this case, all possible relaxation mechanisms other than dissociation must remain negligible (such as Rydberg state fluorescence to the ground state, or subsequent Rydberg state ionization by a further VUV photon). Therefore, the molecule will dissociate sooner or later and the dissociation yield should exactly reflect the absorption probability. This was observed indeed for the G and H states, which both exhibit the same H atom yield[18] and the same C_2H fragment fluorescence,[15] in agreement with their equal absorption cross section.[6,13] In such nonpolarized experiments, these two states only differ by their different spectral line width in their absorption or fragment fluorescence excitation spectrum.

The I $^1\Pi_u$ and J $^1\Pi_u$ upper members in the 5s + 4d complex show a similar behavior in the fluorescence experiment carried out at the synchrotron radiation, as shown in Figure 1. The absorption and total visible fluorescence excitation spectra shown in this figure have been recorded at low resolution (about 1 Å) on the SA63 synchrotron beam line. Panels a and b of this figure show identical profiles for the fluorescence excitation spectrum and for the absorption spectrum with a ratio of about 0.6 between the J−X band and I−X band intensities. The calculated absorption spectrum shown in panel c, based on the semi-united atom approximation (see paragraph C below), presents the same ratio, in complete agreement with the experiments. The $^1\Pi_u$ states of this Rydberg complex obviously predissociate completely into the C_2H + H fragments as they do in the 4s + 3d complex. Nevertheless, as shown in the higher resolution spectra of Figure 2a,c, the J state does not undergo such a fast predissociation as the H state. In this figure, both REMPI and fluorescence excitation spectra exhibit similar rotational line widths of the order of 2 cm^{-1} for the I−X band (1.5 cm^{-1} for the fluorescence excitation spectrum) and 3 cm^{-1} for the J−X band. Simulated spectra shown in panels b and d of this figure correspond to the three-photon excitation probability (b) and to the one-photon VUV absorption probability (d), respectively. The comparison between these simulations and the observed spectra assumes that the ionization probability, in the case of the REMPI experiment, and the dissociation probability, in the case of the fluorescence excitation spectrum, do not depend on the rotational quantum number J, which seems to be the case. The best simulations have been obtained with an average rotational temperature of 150 K in the fluorescence excitation spectrum and 180 K in the REMPI spectrum. The 180 K temperature used in the simulation of the REMPI experiment is consistent with the temperature found from the (3 + 1) REMPI spectrum of the G−X transition performed within the same experimental conditions (not shown here). Comparison between intensities of the simulated three-photon spectrum and the experimental REMPI spectrum indicates that predissociation is present and competes with ionization, inducing a weakening of the REMPI signal. Observed line widths in the spectra of Figure 2 confirm predissociation of both I and J states, in the picosecond time scale, that is, a lifetime of the same order of magnitude as that of the G $^1\Pi_u$ state in the 4s + 3d complex. Recent fragment dispersed fluorescence spectra recorded after VUV excitation of Rydberg states of the ns + (n − 1)d series converging to the first IP showed a general trend with increasing excitation energy: the C_2H fragment is formed with increasing internal energy, especially in the bending excitation.[15,19] From the analysis of the two mechanisms observed by H-fragment translational spectroscopy performed in the 4s + 3d complex, it can be concluded that "slow" dissociation mechanisms taking place in the picosecond time scale are accompanied by a large amount of internal energy in the heavy fragment, involving especially large bending excitation. The very fast dissociation observed only in the H $^1\Pi_u$, 3dδ state, seems to be accidental among the ndδ Rydberg series converging to the first IP.

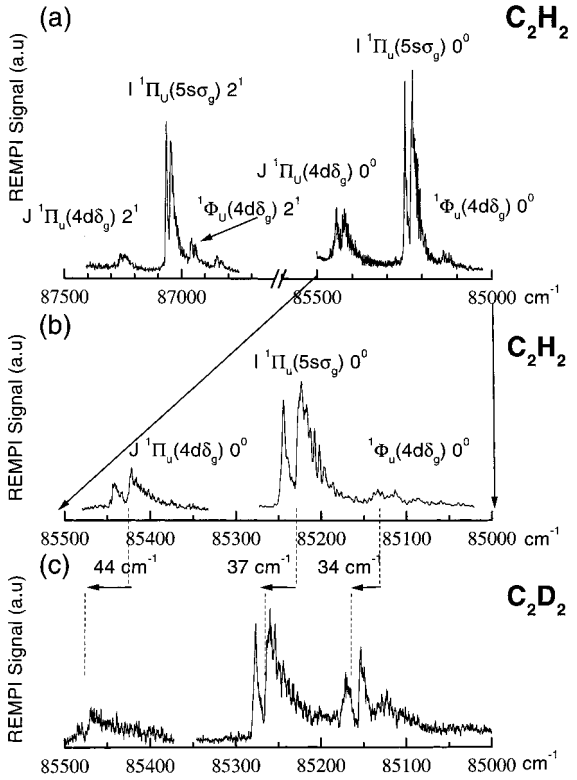

Figure 3. (a) (3 + 1) photon spectrum of C_2H_2 in the region of the 0_0^0 and 2_0^1 bands of the 5s + 4d Rydberg complex. (b) Enlarged region around the origin bands of C_2H_2. (c) Region around the origin bands of C_2D_2. The small positive isotopic shift of 35−45 cm^{-1} is typical of a Rydberg origin band transition.

B. Observation of a New Electronic Component of the 5s + 4d Complex: The 4dδ$^1\Phi_u$ State. The 3dδ component of $^1\Phi_u$ symmetry was first observed by Ashfold et al.,[20] who pointed out that this component was little affected by predissociation. This was later confirmed by Fillion et al.,[10] who calculated the (3 + 1) REMPI spectrum intensity of the corresponding transition as compared to the other members of the 4s + 3d complex. In the REMPI spectrum of the 5s + 4d Rydberg complex shown in Figure 3, a weak feature appears at the expected position for the 4dδ, $^1\Phi_u$ transition, in the origin band region and in the 2_0^1 band region of C_2H_2 (see panel a). This band is much weaker than the I and J bands of the same complex in C_2H_2 and does not exhibit a clear rotational profile as the lower member of the same symmetry did. To positively confirm the assignment of this weak band to the $^1\Phi_u$ component, the isotopomer C_2D_2 REMPI spectrum was recorded under the same conditions and is shown in Figure 3c.

In the later spectrum, the red sideband at 85 150 cm^{-1}, shown in Figure 3c, exhibits a larger intensity than the corresponding one in the C_2H_2 spectrum and could therefore be compared to a three-photon rotational band profile simulation, as shown in the next section and in Figure 5. The most convincing argument for such an assignment still rests on the small and positive isotopic shift of +34 cm^{-1}, typical of a 0_0^0 origin band in the Rydberg spectrum of acetylene (see Table 1). Furthermore, there is no evidence of a similar band in the one-photon absorption spectrum, as expected from the one-photon selection rules.[6] It has to be noted here that the intensity of the 4dδ, $^1\Phi_u$ transition in C_2D_2 is nevertheless unexpectedly strong as compared with our intensity calculations shown in the next section. An overlapping vibronic band in the isotopic spectrum could be responsible for this observed intensity.

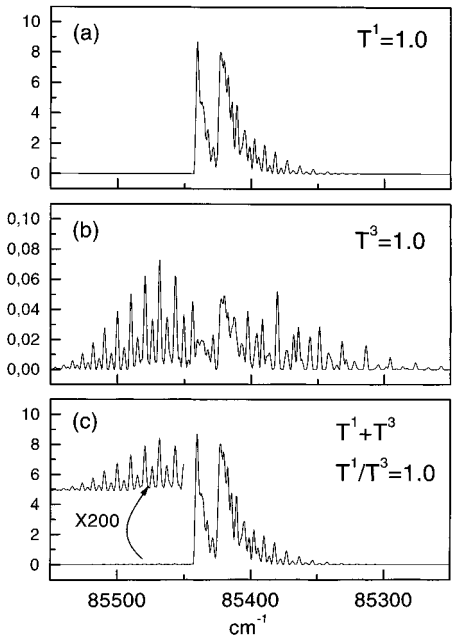

Figure 4. Calculated rotational profile of the J $^1\Pi_u$−X $^1\Sigma_g^+$ three-photon transition assuming a contribution of (a) only the $\mathbf{T}^1$ tensor, (b) only the $\mathbf{T}^3$ tensor, and (c) $\mathbf{T}^1 + \mathbf{T}^3$. The light is linearly polarized and a temperature of 180 K is assumed.

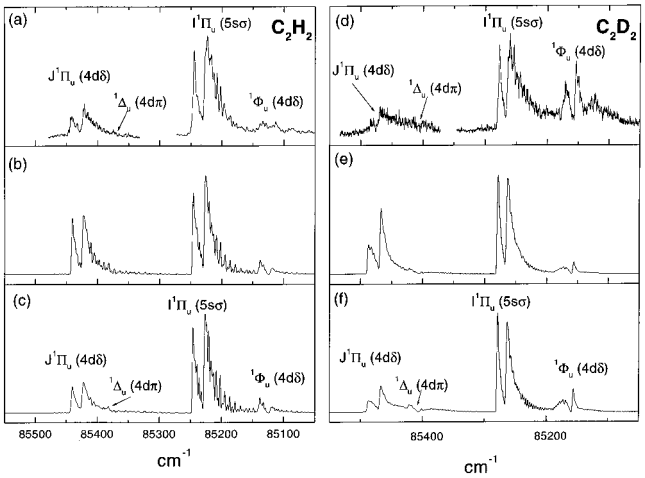

Figure 5. C_2H_2 and C_2D_2 5s + 4d Rydberg complex in the region of 85 000 cm^{-1}: (a), (d) observed (3 + 1) photon ionization spectrum of C_2H_2 and C_2D_2, respectively; (b), (e) calculated three-photon spectrum using the semi-united atom approximation of eq 2 (see text); (c), (f) simulation of the REMPI spectrum by introducing predissociation (see text).

The other three-photon transition, not observable in the one-photon absorption spectrum, concerns the 4dπ, $^1\Delta_u$ Rydberg component. In the observed spectrum of Figure 3b, a very weak feature appears on the red side of the J−X transition. At this point, it is difficult to conclude about the location of the $^1\Delta_u$−X band. To positively locate this transition, we examined the isotopic C_2D_2 spectrum and performed electronic band intensity calculations for the entire Rydberg complex. As will be shown in the next section, we could indeed predict a very weak band corresponding to this $^1\Delta_u$ component in this region, confirmed by the isotopic spectrum (see Table 1 below).

Table 1 summarizes the observed quantum defects for the various observed components of the 5s + 4d Rydberg complex as well as those of the 4s + 3d complex in C_2H_2 and in C_2D_2. These quantum defects show a slight variation from the 3d to the 4d Rydberg states, but nevertheless, confirm the assignment

TABLE 1: Term Values, Quantum Defects and Isotopic Shifts for the Observed Components of the 4s + 3d and 5s + 4d Rydberg Complex

state	C_2H_2		C_2D_2		isotopic shift (cm^{-1})
	T (cm^{-1})	δ	T (cm^{-1})	δ	
$\tilde{F}'\,^1\Phi_u$, $3d\delta_g$[a]	79 931	−0.019	79 976	−0.020	45
$\tilde{G}\,^1\Pi_u$, $4s\sigma_g$[b]	80 111	0.958	80 149	0.958	38
$\tilde{H}\,^1\Pi_u$, $3d\delta_g$[b]	80 458	−0.087	80 475	−0.084	17
$\tilde{H}'\,^1\Delta_u$, $3d\pi_g$[c]	80 640	−0.119	80 661	−0.110	21
$\tilde{F}'\,^1\Phi_u$, $3d\delta_g$ $v_2=1$[a]	81 695	−0.011	81 612	−0.018	−83
$\tilde{G}\,^1\Pi_u$, $4s\sigma_g$ $v_2=1$[b]	81 925	0.960	81 794	0.958	−131
$\tilde{H}\,^1\Pi_u$, $3d\delta_g$ $v_2=1$[b]	82 260	−0.084			
$^1\Phi_u$, $4d\delta_g$[d]	85 131	−0.0053	85 165	−0.0050	34
$\tilde{I}\,^1\Pi_u$, $5s\sigma_g$[b]	85 229	0.965	85 266	0.965	37
$\tilde{J}\,^1\Pi_u$, $4d\delta_g$[b]	85 425	−0.094	85 469	−0.097	44
$^1\Delta_u$, $4d\pi_g$[d]	85 367	−0.076	85 402	−0.076	35
$^1\Phi_u$, $4d\delta_g$ $v_2=1$[d]	86 959	−0.0051			
$\tilde{I}\,^1\Pi_u$, $5s\sigma_g$ $v_2=1$[d]	87 054	0.967			
$\tilde{J}\,^1\Pi_u$, $4d\delta_g$ $v_2=1$[d]	87 250	−0.093			

[a] Reference 20. [b] Reference 6. [c] Reference 10. [d] This work.

of the weak red bands in the spectra of Figure 3 to the 4d $^1\Phi_u$ component in both isotopic species. Isotopic shifts for these Rydberg states transitions are also given in this table, as they provide unambiguous assignments for the Rydberg origin bands. Indeed, all 0_0^0 origin bands exhibit a rather small positive isotopic shift in the range 17−45 cm^{-1}, while vibrational bands involving nonzero vibrational quanta in the Rydberg state correspond to a negative isotopic shift on the order of −100 cm^{-1} or more.

Finally, a question can be addressed about the weakness of this transition as compared to the corresponding well-resolved transition in the lower complex. This has been examined by simulating the REMPI spectra for all components of the 5s + 4d Rydberg complex by using the semi-united atom approximation, as discussed in the next section.

C. REMPI (3 + 1)-Photon Intensity Calculations for the 5s + 4d Rydberg Complex in the Semi-United Atom Approximation. According to Mulliken,[21] the electronic properties of a molecule are in many respects similar to those of the corresponding semi-united atom, i.e., the atom having the same number of electrons as the valence electrons of the molecule. In this description, the 10 valence electrons of acetylene are compared to those of the neon atom with the following correspondence between their ground-state configurations:

$$\begin{aligned} &\text{Ne} && (1s)^2(2s)^2(2p)^6 \\ &C_2H_2 && ...(2\sigma_g)^2(2\sigma_u)^2(3\sigma_g)^2(1\pi_u)^4 \end{aligned} \qquad (1)$$

Comparison between these two configurations suggests a "p" atomic character for the $1\pi_u$ orbital. Therefore, the absorption spectrum of acetylene toward its Rydberg states is expected to be dominated by transitions to *n*s and *n*d states, which is indeed the case with four intense series involving excitation of $ns\sigma_g$ ($^1\Pi_u$), $nd\sigma_g$ ($^1\Pi_u$), $nd\pi_g$ ($^1\Sigma_u^+$), and $nd\delta_g$ ($^1\Pi_u$).[6] In the case of three-photon spectra, other molecular symmetries are allowed by the selection rules, and $nd\pi_g$ ($^1\Delta_u$) and $nd\delta_g$ ($^1\Phi_u$) Rydberg states can also be observed.

By using the semi-united atom approximation, one can evaluate not only the rotational profile of each Rydberg transition, but also the relative electronic radial + angular transition moments within a given *n*s + (*n* − 1)d Rydberg complex. This approximation allows us to predict the relative electronic band strengths of all members belonging to the same Rydberg complex, including s and d orbitals. Concerning the 5s + 4d Rydberg complex, comparison with observed intensities in the absorption spectrum of neon leads to the same radial factor for the electronic transition moments toward the 5s and 4d Rydberg states of acetylene. Molecular Rydberg state symmetry is further taken into account through the angular electronic factor included in the transition moment. This approximation can be applied very easily to the one-photon absorption spectrum of acetylene, as has been done in the calculated spectra of Figures 1c and 2d. When three-photon excitation is considered, some transition intensities involve both one-rank and third-rank tensors, and in this case no direct comparison with three-photon line strengths in Ne is available so far. Nevertheless, one can still use the semi-united atom approximation in order to predict the relative intensities involving the different members of the 4d complex: the $nd\sigma_g$ ($^1\Pi_u$), the $nd\pi_g$ ($^1\Delta_u$), and the $nd\delta$ ($^1\Phi_u$) states. The three-photon line strengths can then be written as follows:

$$I^{(3)}_{l'\lambda'\Lambda'l''\lambda''\Lambda''} \propto N(T,J'')(2J'+1)(2J''+1)\sum_{k=1,3}\left[\sum_p \frac{|T^k_{-p}(\epsilon)|^2}{2k+1}\right]\times \left[\sum_q \mathbf{T}^k(\mu)\begin{pmatrix} l' & k & 1 \\ -\lambda' & q & \lambda'' \end{pmatrix}\begin{pmatrix} J' & k & J'' \\ -\Lambda' & q & \Lambda'' \end{pmatrix}\right]^2 \qquad (2)$$

where $N(T,J'')$ is the temperature dependent rotational population of the ground state and where the first bracket includes the light polarization factor. In the present work, light was linearly polarized, i.e., $p = 0$, leading to polarization weight factors of $^1/_5$ and $^2/_{35}$ for the first-rank tensor and the third-rank tensor contribution, respectively.[22] Within the semi-united atom approximation, the ground-state orbital is considered as a pπ orbital with $l'' = 1$ and $\lambda'' = \pm 1$. The ground state $^1\Sigma_g^+$ molecular symmetry is given by $\Lambda'' = 0$ in eq 2 above. The vibronic tensors $\mathbf{T}^k(\mu)$ are restricted to two parameters $\mathbf{T}^1$ and $\mathbf{T}^3$ containing the radial part of the three-photon transition moment. Since these parameters involve contributions of various unknown three-photon routes in the molecule, their relative weight has to be fitted. Nevertheless, the semi-united atom approximation implies that $\mathbf{T}^1$ and $\mathbf{T}^3$ should keep the same values for all transitions to the 4d states, whatever their molecular symmetry is. This symmetry is taken into account by the electronic and rotational angular factors given by the 3-j symbols in the second bracket of eq 2. Finally, in this approximation, the relative intensities of the three-photon bands involving the I $^1\Pi_u$ $5s\sigma_g$, J $^1\Pi_u$ $4d\delta_g$, $^1\Phi_u$ $4d\delta_g$, and $^1\Delta_u$ $4d\pi_g$ can be simulated all together by fitting only one parameter, the $\mathbf{T}^3/\mathbf{T}^1$ ratio.

Following the approximation leading to eq 2, the rotational intensity profile of the I−X transition only involves the first rank tensor, while the J−X transition intensity involves both $\mathbf{T}^1$ and $\mathbf{T}^3$ tensors, although both transitions have the same symmetry $^1\Pi_u - ^1\Sigma_g^+$. The three-photon transitions ending in the $^1\Phi_u$ $4d\delta_g$ and $^1\Delta_u$ $4d\pi_g$ states only involve the $\mathbf{T}^3$ tensor, which the value of which is equal to that of the J−X transition, according to our simple model. Figure 4 shows the separated contributions of both tensors for the case of the J $^1\Pi_u - $X $^1\Sigma_g^+$ transition, which is the only one to involve both rank tensors in this model. With a $\mathbf{T}^3/\mathbf{T}^1$ ratio equal to 1, the contribution of the $\mathbf{T}^3$ tensor to the rotational line strengths of the J−X transition is negligible. Therefore, the J−X transition is expected to show a rotational profile similar to that of the I−X transition and no precise $\mathbf{T}^3/\mathbf{T}^1$ ratio can be extracted from the analysis of the J−X transition. On the other hand, observation of the weak transitions to the $^1\Phi_u$ $4d\delta_g$ and $^1\Delta_u$ $4d\pi_g$ states indicates that the third rank tensor $\mathbf{T}^3$ has a nonzero value. We therefore have set the $\mathbf{T}^3/\mathbf{T}^1$ ratio to 1 in the three-photon transitions involving

TABLE 2: Parameters Used for the Relative Intensity Calculation of the (3 + 1) Spectrum of the (5s + 4d) Rydberg Complex of C_2H_2 (See the Text)

	5s I $^1\Pi_u$	4d J $^1\Pi_u$	4d $^1\Phi_u$	4d $^1\Delta_u$
$\mathbf{T}^1$	1	1	0	0
$\mathbf{T}^3$	0	1	1	1
$k_i/(k_i + k_p)$	1	0.5	1	1

all members of the 4d Rydberg complex, since this ratio leads to reasonable intensities for the various electronic components of the 5s + 4d complex.

Figure 5 shows the resulting simulated three-photon spectra in comparison with the observed spectrum, in panels a, b, and c for C_2H_2. Similar results are shown for C_2D_2 in Figure 5d−f. The calculated band intensities without considering any predissociation effect are shown in Figure 5b,e. In Figure 5c,f, predissociation has been taken into account by artificially including a damping factor for the ionization signal as follows:

$$s^i = I^{(3)} \frac{k_i}{k_i + k_p} \tag{3}$$

where $I^{(3)}$ is given by eq 2 and k_i and k_p are the ionization rate and the predissociation rate, respectively. The parameters used for the simulations of Figure 5 are given in Table 2.

As shown in Figure 5, the three-photon transitions to the $^1\Phi_u$ 4dδ_g and $^1\Delta_u$ 4dπ_g states are expected to be weak and are very weak indeed in the observed REMPI spectrum. As said above, the $^1\Delta_u$ 4dπ_g−X $^1\Sigma_g^+$ transition barely shows up in the red tail of the J−X transition of C_2H_2 (Figure 5a) and of C_2D_2 (Figure 5d). The small variation of the quantum defect for this electronic component as compared with the lower Rydberg member 3dπ is responsible for the partial overlap of the corresponding transition with the J−X band (see Table 1). Once again, the isotopic shift (given in Table 1) is a signature of an origin band and confirms unambiguously our assignment.

In Figure 5c, the intensity of the J−X transition has been divided by a factor of 2, as compared to the other transitions, especially the I−X transition. We have assumed here, as shown in Table 2, that the predissociation rate k_p is smaller than the ionization rate by at least a factor of 10 and can be neglected in eq 3, for all transitions except the J−X transition. In the latter one, k_i and k_p have approximately the same value, leading to a factor of 2 decrease in the ionization signal. Then, both the decay mechanisms for the J $^1\Pi_u$ 4dδ_g state, ionization and predissociation, compete in the same time scale. The rotational line broadening of about 3 cm^{-1} indicates a lifetime $\tau \geq 1$ ps. This value gives also a reasonable order of magnitude for the ionization time, considering the average power density of the laser beam in the ionization volume and the expected ionization cross section of the Rydberg state.

In conclusion, as in the lower Rydberg complex 4s + 3d, the weakness of the REMPI bands to the Rydberg states $^1\Phi_u$ 4dδ_g and $^1\Delta_u$ 4dπ_g is very well understood in terms of unfavorable three-photon transition moments (electronic + rotational) within the semi-united atom approximation.

IV. Conclusion

New components of the 5s + 4d Rydberg complex have been experimentally characterized by their (3 + 1) REMPI spectrum in both isotopic C_2H_2 and C_2D_2. The relative intensities of the corresponding electronic transitions have been interpreted in the semi-united atom approximation, by taking into account moderate predissociation in the picosecond time scale. In comparison with the lower 4s + 3d Rydberg complex, the overall intensity of the observed transitions is significantly weaker and follows an approximate scaling law of about $(^4/_5)^3$, as observed in the absorption spectrum of neon and expected for molecular Rydberg states.

In addition to this weakening of the REMPI signal with increasing principal quantum number *n*, predissociation also contributes to the decrease of the ionization signal from the acetylene Rydberg states. To explore the structure and the stability of the higher members of the s and d Rydberg series, a better approach than one-color REMPI spectroscopy consists of detecting the photofragmentation products by their fluorescence. This technique has been applied here by using a very high-resolution VUV excitation by synchrotron radiation,[16] allowing for rotational resolution of the Rydberg bands and rotational spectral line width measurements. The use of the synchrotron line beam allowed us to observe over a very large spectral range the complete Rydberg series of acetylene converging to the first IP, as shown elsewhere.[15,19]

Predissociation is more the rule than the exception for all Rydberg states of acetylene. Most of the electronic components of the 4s + 3d and 5s + 4d Rydberg complexes predissociate in a time scale of 1−10 ps, except for the H $^1\Pi_u$ 3dδ state, which dissociates in the femtosecond time scale. This very fast decay probably proceeds through an accidental crossing in the potential energy surface of the H state and should be confirmed by accurate ab initio calculations in the 10 eV region. The other Rydberg states converging to the first IP seem to show a smooth behavior toward predissociation, leading to C_2H fragments in their excited A state, which fluoresce in the infrared and visible region. In astrophysical media, as circumstellar envelopes, the VUV photodissociation of acetylene between 8 and 11.4 eV (which is the most relevant spectral region for the interstellar flux) is then mainly producing C_2H and H. We have shown here that this fragmentation mostly proceeds through predissociation of Rydberg states and essentially leads to an electronically excited and vibrationally hot ethynyl radical, which further relaxes radiatively into the ground state.

Acknowledgment. This work has been partially supported by the Programme National "Physique et Chimie du Milieu Interstellaire" and by the "Programme National de Planétologie" (CNRS). We are grateful to Pr. Ph. Bréchignac and Pr. S. Couris for their help and useful discussions during the experimental stage at the synchrotron radiation. We also thank M. Bonneau for his technical assistance during all the experiments. A.C. and C.F. acknowledge a Brazilian government (CAPES) visiting grant and a CNRS scientist visiting position (C.F.).

References and Notes

(1) Hsu, Y. C.; Lin, M. S.; Hsu, C. P. *J. Chem. Phys*. **1991**, *94*, 7832.
(2) Han, J. C.; Ye, C.; Suto, M.; Lee, L. C. *J. Chem. Phys*. **1989**, *90*, 4000.
(3) Cool, T.; Goodwin, P. *J. Chem. Phys.* **1991**, *94*, 6978.
(4) Wang, J. H.; Hsu, Y. T.; Liu, K. *J. Phys. Chem.* **1997**, *101*, 6593.
(5) Löffler, P.; Wrede, E.; Schnieder, L.; Halpern, J. B.; Jackson, W. M.; Welge, K. H. *J. Chem. Phys.* **1998**, *109*, 5231.
(6) Herman, M.; Colin, R. *Phys. Scr*. **1982**, *25*, 275.
(7) Glassgold, A. E. *Annu. Rev. Astron. Astrosphys*. **1996**, *34*, 241.
(8) Crovisier, J. *Faraday Discuss.* **1998**, *109*, 437.
(9) Ashfold, M. N. R.; Tutcher, B.; Yang, B.; Jin, Z. K.; Anderson, S. L. *J. Chem. Phys.* **1987**, *87*, 5105.
(10) Fillion, J. H.; Campos, A.; Pedersen, J.; Shafizadeh, N.; Gauyacq, D. *J. Chem. Phys.* **1996**, *105*, 22.
(11) Laruelle, F.; Lievin, J. Manuscript to be published.
(12) Orlando, T. M.; Anderson, S. T.; Appling, J.; White, M. G. *J. Chem. Phys.* **1987**, *87*, 852.

(13) Shafizadeh, N.; Fillion, J. H.; Gauyacq, D.; Couris, S. *Philos. Trans. R. Soc., London A* **1997**, *355*, 1637.

(14) Guizard, S.; Shafizadeh, N.; Horani, M.; Gauyacq, D. *J. Chem. Phys.* **1991**, *94*, 7046.

(15) Campos, A.; Boyé, S.; Bréchignac, Ph.; Douin, S.; Fellows, C.; Shafizadeh, N.; Gauyacq, D. *Chem. Phys. Lett.* **1999**, *314*, 91.

(16) Nahon, L.; Alcaraz, Ch.; Marlats, J.-L.; Lagarde, B.; Polack, F.; Thissen, R.; Lepère, D.; Ito, K. *Rev. Sci. Instrum.* **2001**, *72*, 1320.

(17) Douin, S.; Campos, A.; Boyé, S.; Bréchignac, Ph. Manuscript to be published.

(18) Löffler, P.; Lacombe, D.; Ross, A.; Wrede, E.; Schnieder, L.; Welge, K. H. *Chem. Phys. Lett.* **1996**, *252*, 304.

(19) Boyé, S.; Campos, A.; Douin, S.; Fellows, C.; Gauyacq, D.; Shafizadeh, N.; Halvick, Ph. Manuscript to be published.

(20) Ashfold, M. N. R.; Dixon, R.; Prince, J.; Tutcher, B. *Mol. Phys.* **1985**, *56*, 1185.

(21) Mulliken, *R. Intern. J. Quantum Chem*. **1967**, *1*, 103.

(22) Dixon, R.; Bayley, J.; Ashfold, M. N. R. *Chem. Phys.* **1984**, *84*, 21.